metals

MDPI

Article

Joining of Macroscopic 3D Steel Transition Wire Structures to Steel Sheets: Study on the Mechanical, Microstructural, and Phase Characteristics of Brazed and Glued Joints

Saravanan Palaniyappan [1,*], Andreas Todt [1], Maik Trautmann [1], Felix Röder [2], Carolin Binotsch [2], Birgit Awiszus [2] and Guntram Wagner [1]

[1] Group of Composites and Material Compounds (PVW), Institute of Materials Science and Engineering (IWW), Chemnitz University of Technology, 09125 Chemnitz, Germany; andreas.todt@mb.tu-chemnitz.de (A.T.); maik.trautmann@mb.tu-chemnitz.de (M.T.); guntram.wagner@mb.tu-chemnitz.de (G.W.)

[2] Group of Virtual Production Engineering (ViF), Chemnitz University of Technology, 09125 Chemnitz, Germany; felix.roeder@mb.tu-chemnitz.de (F.R.); carolin.binotsch@mb.tu-chemnitz.de (C.B.); birgit.awiszus@mb.tu-chemnitz.de (B.A.)

* Correspondence: saravanan.palaniyappan@mb.tu-chemnitz.de; Tel.: +49-371-531-33873

Abstract: With an increased demand for the combination of different material classes in lightweight applications like automobiles, aircraft construction, etc., the need for simple and energy-efficient joining technologies to join these different material classes has been extensively researched over the last decades. One such hybrid material combination is the metal–plastic hybrid structure, which offers the combinational characteristics of high strength and stiffness of the metal part along with characteristic elasticity and low density of the plastic part. In this research work, the focus is laid on generating a graded property transition at the interface of metal–plastic joints by brazing a three-dimensional (3D) macroscopic transition wire structure (TWS) strucwire®, over the metal part before being molded with plastic at a later stage using an injection over-molding process. This helps in providing a mechanical interlocking facility and thereby achieving a higher load transfer at the interface of metal–plastic hybrid joints. The graded steel wire structures with different carbon content were brazed onto the galvanized steel sheets using the hotplate brazing technique. In addition to the Zinc layer on the galvanized steel sheets, electroplated Zinc coatings were fabricated on the wire structures to provide better brazing quality. The microstructural, mechanical, and intermetallic phase characteristics of the resulting brazed joints were evaluated using light microscopy, adhesion tests, and scanning electron microscopy, respectively.

Keywords: 3D transition wire structure; steel wire brazing; electroplated Zn coating; pull-off adhesion test; SEM; contact angle

Citation: Palaniyappan, S.; Todt, A.; Trautmann, M.; Röder, F.; Binotsch, C.; Awiszus, B.; Wagner, G. Joining of Macroscopic 3D Steel Transition Wire Structures to Steel Sheets: Study on the Mechanical, Microstructural, and Phase Characteristics of Brazed and Glued Joints. *Metals* **2022**, *12*, 1116. https://doi.org/10.3390/met12071116

Academic Editor: António Bastos Pereira

Received: 28 April 2022
Accepted: 27 June 2022
Published: 29 June 2022

1. Introduction

As a result of an ongoing need and continuously growing prevalence for lightweight engineering structures in almost every application, including automobile, aircraft, healthcare industries, etc., the necessity to join dissimilar materials, in particular metal–plastic structures, is gaining a lot of importance [1,2]. Such a combination of different materials in lightweight construction has led to the growing importance of mixed construction of metal–plastic compounds. These mixed constructions are usually characterized by an additional joining zone at the interface between the two dissimilar materials that form the structural and functional unit of the complete metal–plastic compound [3]. The ultimate aim of joining such dissimilar materials together is to enhance the flexibility of product design and thereby allowing the possibility to use various properties in a combined manner. In this way, the separate properties of the combining materials are utilized efficiently and functionally [1]. This occurs as a result of the properties of both dissimilar materials

complementing each other to deliver an outstanding structural performance that could not be delivered by each of the two dissimilar materials independently [4].

There are several available technologies to join metal–plastic hybrid compounds that could generally be grouped into one of the following three methodologies, i.e., mechanical clamping on the microscale, coating of the semi-finished products to be injected, and the chemical modification of the thermoplastic [5]. Owing to the potential disadvantage of the stress concentration near the rivet zone when using mechanical fastening and riveting techniques, the classical in-mold assembly and post-mold assembling techniques were introduced later in [6–8]. Then again, these technologies were being introduced with additional post-processing stages, such as clinching [9,10], ultrasonic hot air stacking, etc. [4,11], that further increased the complexity of hybrid metal–plastic compound production processes. For these reasons, the over-molding of plastic to metal structures through the injection molding process has been used as a versatile method since then. This holds the advantage of combining the production and joining of plastic with metal sheets in a single-stage operation [12]. The successful implementation of metal–plastic hybrid compounds was first realized in the late 1990s by over-molding steel sheets with elastomer modified glass fiber reinforced Polyamide (Durethan BKV 130; PA6-GF30) at the front end of the Audi A6 [4]. Following such classic macro form-fit technologies, many new processes for micro form-fit processes through over-molding have been researched over the last few decades [13]. Several other innovative technologies like laser micro structuring on the metal surface [12,14], the mechanical interlocking effect [15,16], electrochemical treatment of metal inserts [17], fiber laser joining [18,19], and laser transmission joining [20], etc., have also been used to attain metal–plastic joints using a variety of different categories of metals and plastics. Although many researchers focused innovatively on joining metal–plastic components using various novel methodologies and technologies, the core problem of sudden property variation in the joining zone has not been elaborately discussed so far.

When joining metal–plastic components using any of the above-mentioned technologies, including over-molding, the problem of sudden property difference at the interfacial joining zone arises. This property difference in terms of strength, elastic modulus, thermal expansion, etc., can have a negative impact not only on the behavior of hybrid metal–plastic compounds but also influences the effectiveness of the manufacturing process and the usage of end product [21]. In addition, as a result of insufficient or weaker bonding between the metal–plastic hybrid compounds, the mechanical strength of the base material is not fully utilized to its highest potential. This is because of the transfer or absorption of the mechanical or thermal stresses by the mechanically weaker plastic part, which ultimately fails at an early stage [5,21].

To overcome these problems, a novel three-dimensional (3D) macroscopic metal wire transition zone could be designed and introduced between the sheet metal and the plastic component to achieve a graded property transition with significantly higher loads. A schematic of such a hybrid metal–plastic structure is shown in Figure 1.

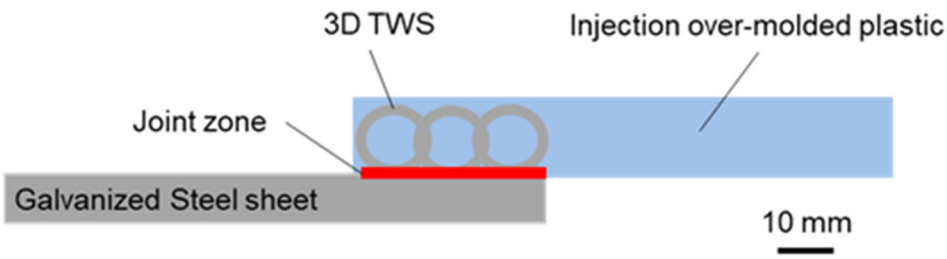

Figure 1. Schematic of the project outcome: A hybrid metal–plastic compound structure with a 3D macroscopic transition zone at the interface.

This is an expected outcome of this ongoing project, and the experimental results and characterizations of the injection-molded metal–plastic hybrid structures are already in the progress of being published as a separate article. In this ongoing research work,

the 3D permeable transition wire structures (strucwire®) are used to realize the intended graded transition property in the metal–plastic joining zone. To connect the transition structures with the metal component, the material joining process called hot plate brazing, which allows efficient application and high resilience is used. The brazed steel–steel wire structures are then converted into hybrid compounds by over-molding the permeable transition structure using thermoplastic melts through the injection molding process.

This article focuses mainly on the joining (brazing and adhesion bonding) of 3D metal wire structures to the base of a galvanized steel sheet followed by the relevant microstructural and phase analyses of the joint zone using light microscopy and energy-dispersive X-ray spectroscopy in scanning electron microscopy, respectively.

2. Experimental Procedures

2.1. Materials and Methods

In the first step of determining the suitable brazing alloy for steel–steel joints, the literature provided numerous possibilities, which are not limited to Silox S6S (AlSi), Silox S7A (CdZn), Fontargen A636 (ZnAl), Fontargen AF631NH (ZnAl), etc. Of these, the above-mentioned set of brazing alloys were selected and applied to the surface of galvanized steel sheets in air and argon (Ar) atmospheres separately. Using the same experimental conditions, two steel sheets were also brazed together with these brazing alloys placed in between the two steel sheets. For each brazing alloy, a minimum of three experiments were conducted to ascertain the reproducibility and repeatability of the joining property. The contact angle measurements were then performed on the obtained microscopical images to determine the wettability of different brazing alloys on the steel sheet surface. The results and analyses of all other brazing alloys are purposely omitted and only the results of brazing alloy L1 are elaborately discussed in this article. It shows stable bonds with the Zn coating of the steel sheets by solid solution phases.

For manufacturing steel sheets to steel–wire joints, galvanized micro-alloyed steel sheets (HX340 LAD;1.0933) with dimensions of 100 × 25 × 0.8 mm^3 and 3D transition wire structures (Kieselstein GmbH, Chemnitz, Germany) with dimensions of 100 × 25 × 5 mm^3 are used as base materials. A schematic of the lap joint setup is shown in Figure 2.

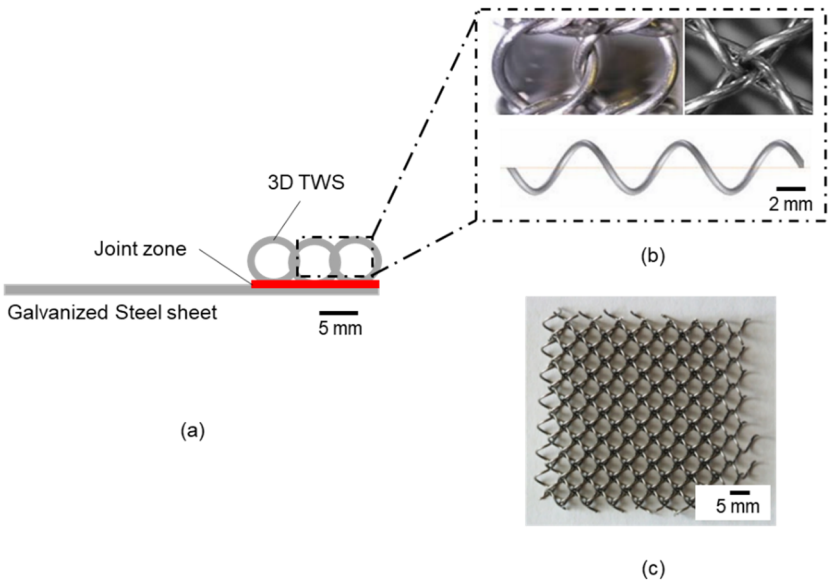

Figure 2. (**a**) Schematic setup of the brazed lap joint, (**b**) magnified view of 3D TWS strucwire®, (**c**) top view of the 3D TWS with permeable regions visible.

To achieve the graded property transition in the interfacial joint zone of metal–plastic hybrid structures, three different 3D transition steel wire structures with variable carbon

content were used. Detailed material composition and dimensional specifications of the three different TWS are provided in Table 1.

Table 1. Material composition and dimensional specifications of the 3D TWS strucwire®.

Sample ID	Material Group	DIN/EN Number	Carbon Content	Single Wire Diameter	Permeable Cell Size
(–)	(–)	(–)	(wt.%)	(mm)	(mm)
C75	Spring steel	1.0605	0.70–0.80	0.63	4.7
C62D2	Spring steel	1.1222	0.60–0.64	0.60	
C50	Tempered steel	1.1206	0.50		

The lap joints were produced by using either brazing alloy (L1) or adhesive paste (K1) separately for each set of experiments and the results were comparatively analyzed. As the brazing alloy L1, Fontargen AF631 NH (Sonderlote, Eisenberg, Germany) was used, and as the adhesive paste K1, Toolkraft EPO5.K50 adhesive (Conrad Electronic SE, Hirschau, Germany) was used. A summary of the properties of both L1 and K1 is given in Table 2.

Table 2. Properties of brazing alloy L1 and adhesive paste K1.

Sample ID	Material Type	Product Name	Chemical Composition	Working Temperature	Temperature Resistance	Post Curing
(–)	(–)	(–)	(–)	(°C)	(°C)	(–)
K1	Adhesive	TOOL CRAFT—Two Component Epoxy adhesive (EPO5.K50)	Epoxy resin + Hardener	RT	~120	25 °C/48 h
L1	Brazing alloy	Fontargen AF631 NH	Zn98Al solder rods with flux core	382–417	-	-

Before brazing, the 3D TWS were manually cut into the dimension of 25 × 25 × 5 mm^3, and along with the pre-cut galvanized steel sheets, they were pre-treated in an ultrasonic acetone bath at 50 °C for 15 min. The brazing process was carried out in atmospheric air, and the course of the complete brazing process is depicted in Figure 3.

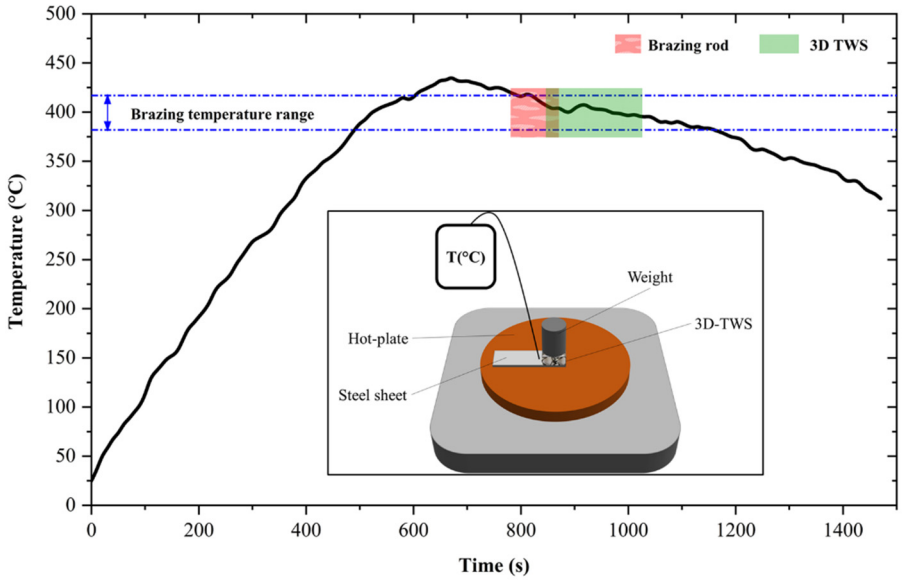

Figure 3. Process flow (temperature vs. time) and the experimental setup (inset) of brazing 3D TWS to galvanized steel sheets using L1 on a hot plate.

Theoretically, the zinc layer on the galvanized steel could be used to connect the 3D transition structure. However, an additional Zinc coating onto the transition wire structures was fabricated through the electroplating process to study the effect of Zn coating on the bonding mechanism of the brazing process. The electroplating of Zn was carried out only on the C75 type transition structures that were hot, degreased, and decantated with dilute sulphuric acid (H_2SO_4) before electroplating. The electroplating process was carried out using rack plated 3D transition wire structures dipped in an alkaline Zinc electrolyte solution at 25 °C for five different coating times of 5 min, 15 min, 30 min, 45 min, and 60 min. The current density was maintained at 2.5 A/m^2 throughout the process.

2.2. Characterization Techniques

2.2.1. Pull-Off Adhesion Test

For testing and comparing the adhesion quality of the brazed joints with the glued joints, pull-off adhesion tests were conducted on two variants. Based on DIN EN ISO 4624:2014-06, the samples were prepared using two steel blocks for each specimen with/without 3D TWS in the middle, joined by using either the adhesive paste (K1) or the brazing alloy (L1). The schematic of the pull-off test specimens is shown in Figure 4.

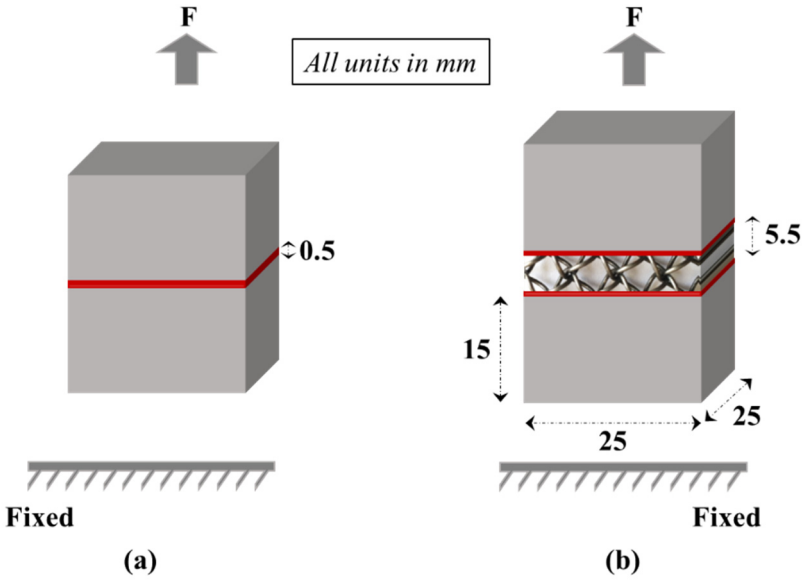

Figure 4. Schematic setup of (**a**) the steel block joint without 3D TWS and (**b**) the steel block joint with 3D TWS used in the pull-off adhesion test to determine the adhesion strength of L1 and K1.

The adhesion tests were carried out at room temperature using a Zwick All-round-Line 20 kN (Zwick-Roell GmbH & Co., KG, Ulm, Germany) tensile testing device. The main reason behind using steel blocks instead of steel sheets is to be able to grip the adhesion test samples on both sides using the clamping unit of the tensile testing device. The samples were pre-stressed until 2 N and then the tests were conducted with an elongation speed of 1 mm/min until the fracture of the brazed or glued joint. The relevant adhesion strengths of the joints were calculated and comparatively analyzed.

2.2.2. Light Microscopy and Scanning Electron Microscopy

The cross-sections of the steel–TWS joint zone were prepared metallographically through the warm embedding of the brazed and glued samples separately in epoxy resin, followed by grinding and polishing. The light microscopy images were recorded using a stereo light microscope OLYMPUS GX51 (Olympus Europa SE & Co. KG, Hamburg, Germany) inbuilt with the OLYMPUS STREAM digital image acquisition and processing technology. For the microstructural and phase analyses of the brazed steel–TWS structures, a scanning electron microscope ZEISS LEO1455VP with X-ray micro range analysis EDAX GENESIS from Carl

Zeiss (Oberkochen, Germany) was used. For the SEM analyses, the polished surfaces of the cross-sections were pre-coated with a very thin layer of Carbon using an Emitech K450 (Quorum Technologies Ltd., Laughton, UK) Carbon evaporation coater.

2.2.3. X-ray Diffractometry

XRD phase analyses on the galvanized steel sheets along with non-coated and Zn-coated steel transition wire structures were carried out using a diffractometer (Bruker, D8 Discover, Karlsruhe, Germany) with Co–K radiation. The XRD samples were analyzed using a point focus beam through a 0.5 mm pinhole aperture and a LynxEye XE—T detector (Bruker, Karlsruhe, Germany) for a measurement time of approximately 24 h.

3. Results and Discussions

3.1. Contact Angle Analyses on L1 Joints

By analyzing the obtained microstructural images of steel–steel joints, it was determined that the contact angle of Fontargen AF631NH (L1) was found to be around $8 \pm 5^{\circ}$ and $15 \pm 6^{\circ}$ in atmospheric air and argon, respectively. When analyzing the brazing alloy between two steel sheets, the brazing alloy was evenly distributed and the structural joint was firm for joints brazed in atmospheric air. However, in the argon atmosphere, the brittleness of the joint zone increased, and the structural joints were much weaker than the joints produced in atmospheric air conditions. This is shown in the illustrations. However, the cause is still unknown. The microscopic images of both argon and air-brazed L1 steel–steel joints are shown in Figure 5.

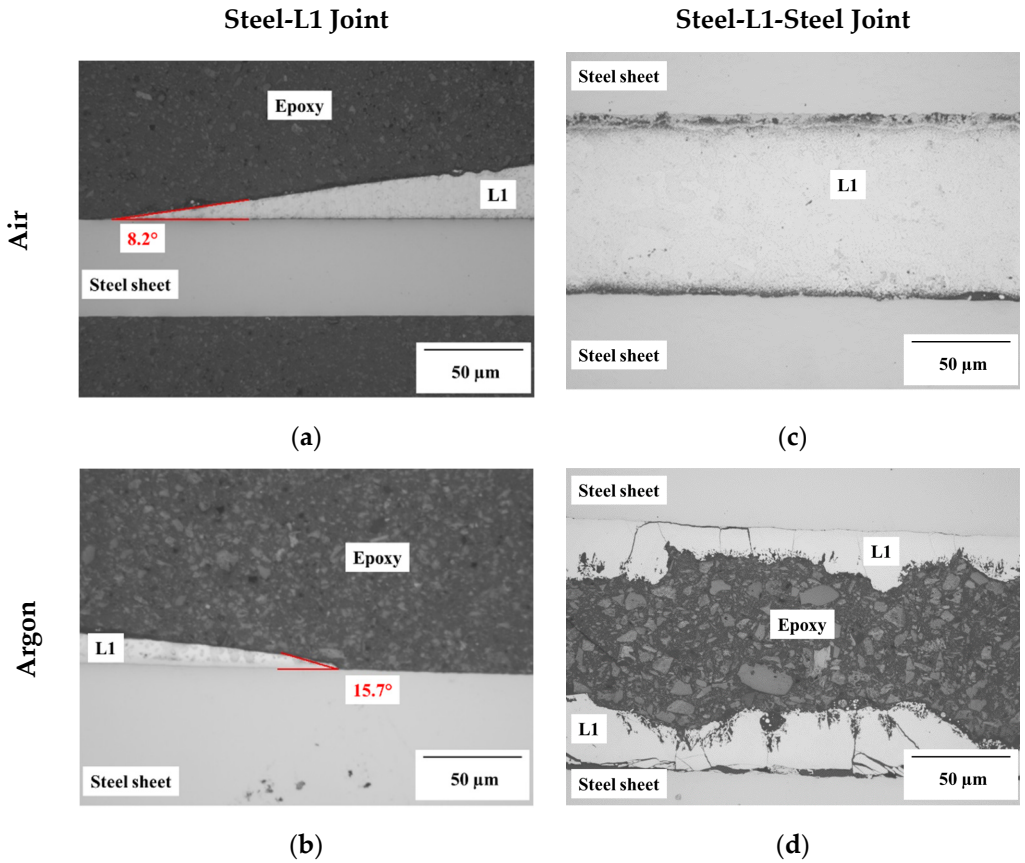

Figure 5. Light microscopy images of steel–L1 and steel–L1–steel brazed joints in air and Ar atmosphere. (**a**) Steel–L1 joint zone in air, (**b**) steel–L1 joint zone in Ar for contact angle analyses, (**c**) steel–L1–steel joint zone in air, (**d**) steel–L1–steel joint zone in Ar.

3.2. Brazing Alloy (L1) vs. Adhesive Paste (K1)

The light microscopy images of brazed and glued joints of the steel sheet–3D TWS are shown in Figure 6.

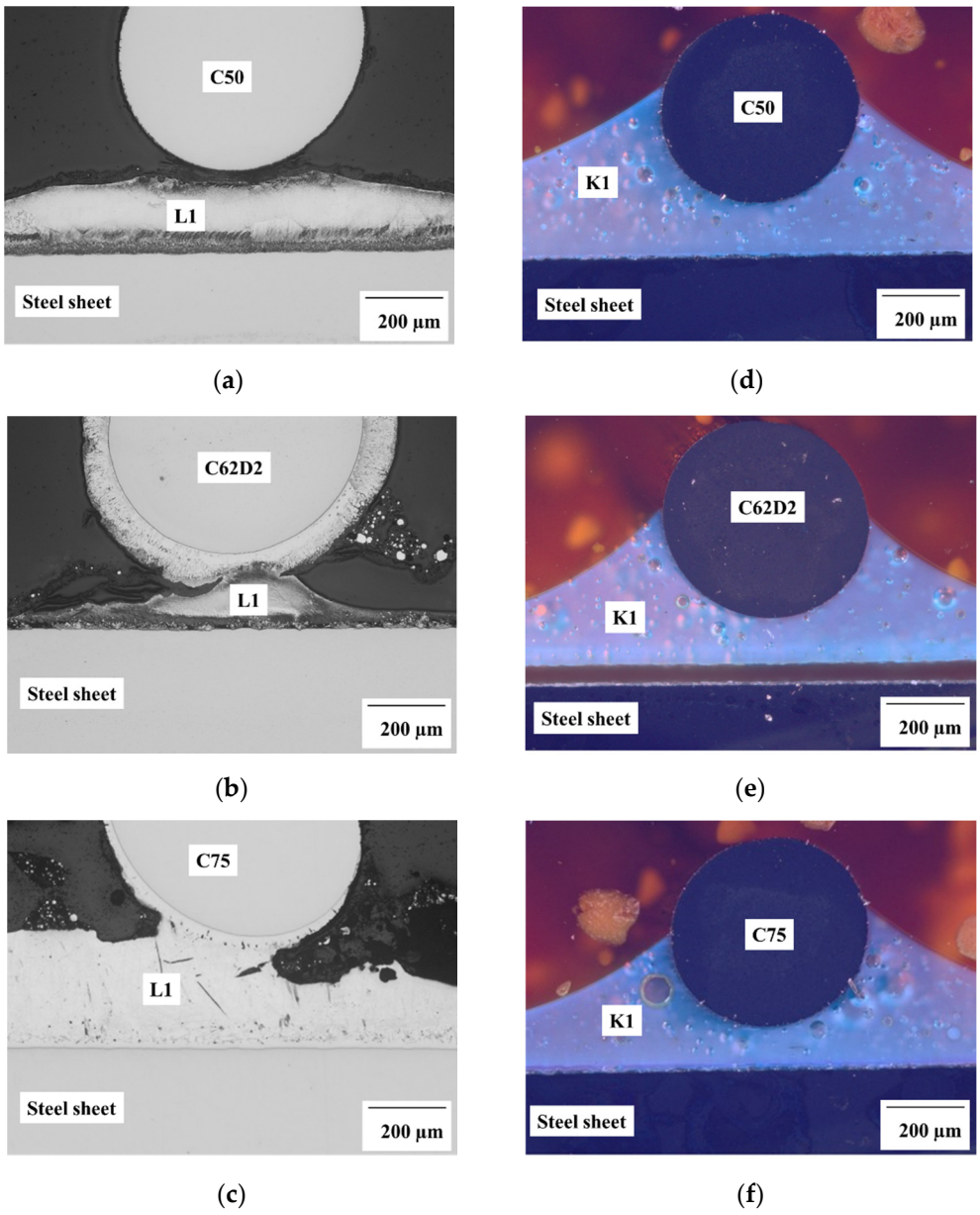

Figure 6. Light microscopy images of the L1 brazed (**a**–**c**) and the K1 adhesive glued (**d**–**f**) steel sheet–L1/K1–TWS joints using all the three different TWS.

In terms of brazed joints, the bonding between the TWS and the steel sheets is limited to a smaller area of contact. This is because of the cylindrical dimension of the TWS that comes into contact with the steel sheet over the brazing alloy L1 at a smaller surface area. However, regarding the glued joints, the bonding is better with the glue flowing around half the circumference of the TWS. This provides a more stable bonding of the TWS to the flat steel sheets. Additionally, it should be mentioned here that some of the cross-sectional images show a debonding of the TWS from L1 (Figure 6a) or debonding of the glue K1 from the steel sheet (Figure 6e). This occurred during the metallographic preparation of the cross sections and should not be confused with the bonding of the adhesive and braze. The same bonds were stable before the cross-section preparation.

This means that the bond strengths are very low, and the perfect characterization is still to be considered complex.

Upon analyzing the adhesion strength of K1 and L1 when glued and brazed, respectively, in the process of preparing steel sheet–L1/K1–TWS joints, it was observed that the glued joints evidenced a greater adhesion strength from 0.20 to 0.34 MPa and the brazed joints evidenced a lower adhesion strength from 0.008 to 0.014 MPa, depending on the type of TWS was used. In the case of steel sheet–steel sheet joints without any TWS in between (as shown in Figure 4a), the brazed and glued joints provided an adhesion strength of 0.28 ± 0.2 MPa and 3.20 ± 0.40 MPa, respectively. With an increase in the carbon content of the TWS, there was an increase in the adhesion strength of both glued and brazed joints. This is attributed to the higher carbon content that assists in the process of bonding between the joints. However, there is no significance because the base materials are similar, and the carbon content does not appear to have a significant effect. A summary of the adhesion strength of K1 and L1 joints with the TWS zone is given in Figure 7.

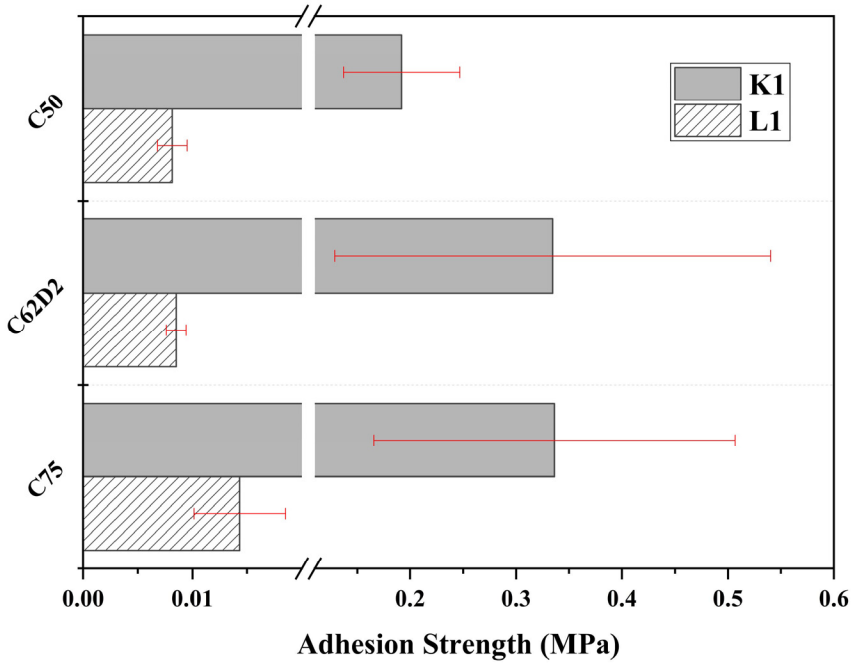

Figure 7. A comparative plot of the adhesion strength analyses on L1 and K1 joints based on the pull-off adhesion tests.

3.3. Effect of Zinc Coating on 3D-TWS

To improve the brazing quality, an additional Zn coating on the C75 TWS was fabricated through the electroplating of Zn. The thickness of the Zn coating increased with an increased coating time at a growth rate of around 0.38 µm/min. The XRD diffractogram of the Zn coating showed the same crystallographic phases of the Zn that was already available on the galvanized steel sheets. The variation of the thickness of the Zn coating with the relevant light microscopic images, along with the XRD diffractograms (inset) of the non-coated C75, 60-min Zn coated C75, and galvanized steel sheets, is shown in Figure 8.

The Zn coating provided comparatively more attraction of the L1 alloy to the TWS. This occurred because of the Zn ions present in the L1 brazing alloy, which have more affinity towards the Zn-coated TWS than the non-coated TWS. The Zn affinity also increased as the Zn coating thickness increased with the coating time. Several intermetallic phases were also formed during this process, and these are elaborately discussed in the following Section 3.4. The light microscopic images of the steel sheet–L1–Zn/C75 joints obtained using three different coating thicknesses are shown in Figure 9.

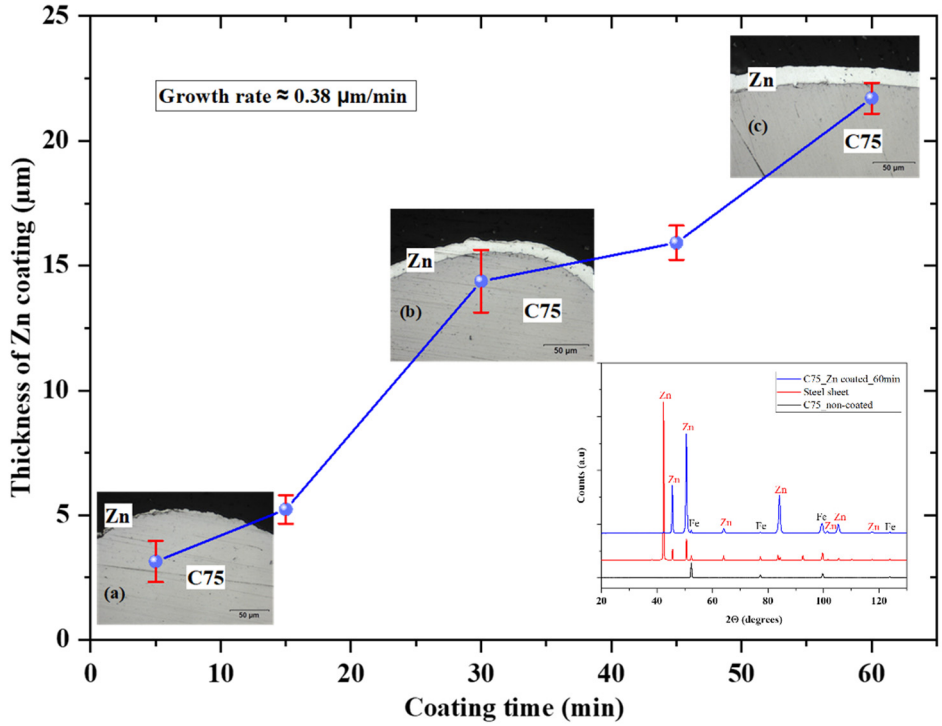

Figure 8. Thickness variation and light microscopy images of (**a**) 5 min, (**b**) 30 min, and (**c**) 60 min coated Zn layer on C75 TWS. Inset: XRD diffractogram of Zn coated C75 compared with the diffractograms of non-coated C75 and galvanized steel sheet.

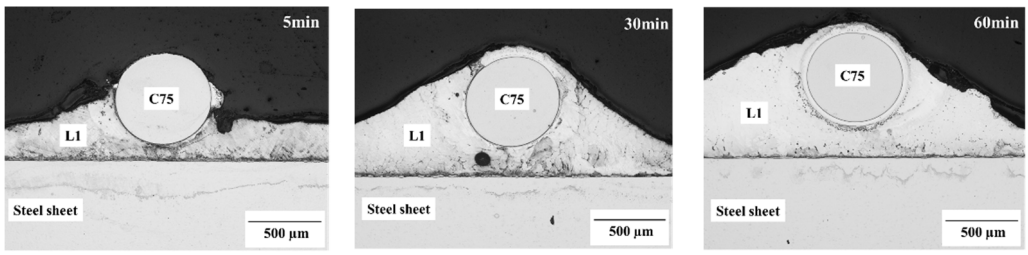

(**a**) (**b**) (**c**)

Figure 9. Light microscopy images of brazed steel sheet–L1–Zn coated C75 TWS joints with (**a**) 5 min, (**b**) 30 min, and (**c**) 60 min Zn electroplating time.

The influence of the Zn content on the mechanical properties of the compounds is currently under investigation. Relevant results on this are expected with regard to the joint strength.

3.4. EDX Phase Analyses

The elemental characterizations of one type of TWS (C62D2) and Zn coated C75 brazed to galvanized steel sheets were performed in the SEM equipped with EDX. Upon analyzing the interface between the steel sheet and the brazing alloy L1, the intermetallic phases of hexagonal close-packed (hcp) Zn + δ FeZn were observed closer to the steel sheet, and the phase of hcp Zn + ζ FeZn was observed a little farther from the steel sheet (δ FeZn: $Fe_{0.64}Zn_{10.48}$; ζ FeZn: $FeZn_{13}$). A combination of both δ FeZn + ζ FeZn was observed at the interface region between the brazing alloy L1 and the 3D TWS C62D2. It should also be noted that a thin interfacial layer of δ FeZn was observed without any ζ FeZn phase very near to the C62D2 TWS. In the case of Zn-coated C75 TWS that were brazed using L1, the diffusion of αFe from the C75 TWS was observed in the Zinc coating along with the hcp

Zn phase. At the brazing alloy region, along with the face-centered cubic (fcc) Aluminum phase of the alloy, there a diffusion of Fe from the galvanized steel sheet into the brazing alloy appeared, leading to the formation of the Fe_4Al_{13} phase. The SEM microstructural images of the interfacial zones along with the marked EDX analyzed phase compositions are shown in Figure 10.

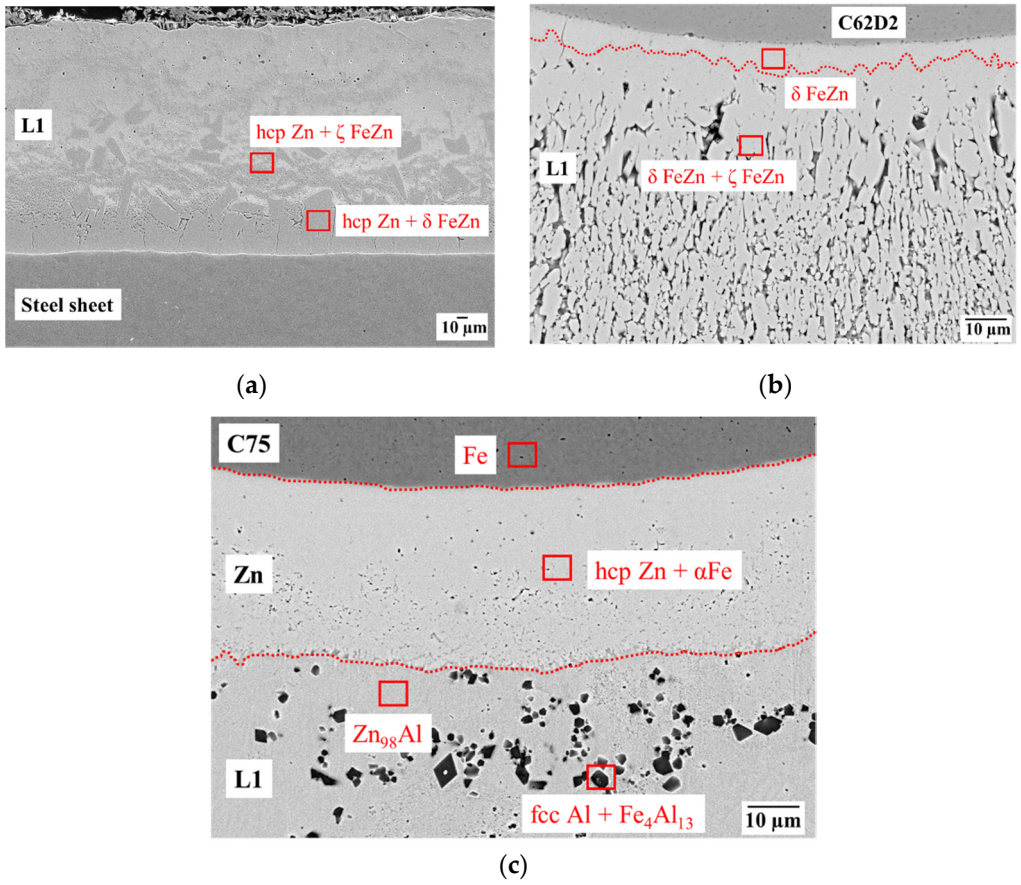

Figure 10. EDX phase analyses on the interphase of (**a**) C62D2-L1, (**b**) L1–Steel sheet, and (**c**) C75-Zn coating–L1 regions.

4. Conclusions

To introduce and execute a macroscopically graded property transition at the joining surface of metal–plastic hybrid joints, this article mainly focuses on the mechanical, microstructural, and phase transition properties of brazed metal 3D TWS joints, and some of the results are compared with bonded joints to show the differences. In terms of mechanical bond strength, the bonded joints were found to be stronger with a strength almost 13 times higher than the brazed joints. This is due to the curvature of the cylindrical circumference of the TWS, which is in contact with the steel sheet and provides only a limited surface area for bonding. With adhesive bonds, this surface area of the TWS in contact with the steel sheet is increased by the improved flowability of the adhesive, which flows and embeds almost half of the circumferential area of the TWS along with the steel sheet. Soldering tests yielded good results with a ZnAl-based solder. The intermetallic phase analyses revealed that Fe diffuses from both the steel 3D TWS and the steel sheets into the interfacial solder zone, leading to the formation of ζ FeZn and δ FeZn phases in the brazing zone. This allows for the good bonding of the two metallic partners. The electroplated Zn coating on the 3D TWS provided improved affinity of the braze to the TWS. During brazing of the Zn-coated TWS, the diffusion of αFe from the TWS into the Zn layer and the formation of the Fe4Al13 phase in the brazing zone by the diffused Fe from the steel sheet were observed. This

results in even better low-stress joints. It was demonstrated that graded structures can be produced with brazing and bonding to produce high-quality joints.

This is an ongoing research effort to develop metal–plastic hybrid composite structures with macroscopically graded property transitions at the interface, and the injection molding results should be published soon.

Author Contributions: Conceptualization, M.T. and C.B.; methodology, C.B., A.T., M.T., S.P. and F.R.; experimental investigations, S.P. and A.T.; data analyses, S.P.; writing—original draft preparation, S.P. and A.T.; writing—review and editing, S.P., A.T., M.T., C.B. and F.R.; material resources, G.W. and B.A.; supervision, M.T., A.T. and C.B.; project administration, G.W. and B.A.; publication funding acquisition, S.P., A.T., F.R., C.B. and M.T. All authors have read and agreed to the published version of the manuscript.

Funding: The research work was funded by the Deutsche Forschungsgemeinschaft (DFG, German Research Foundation) as part of the cooperative project DFG-434351205. The publication of this article was funded by the Chemnitz University of Technology and by the Deutsche Forschungsgemeinschaft (DFG, German Research Foundation) DFG-491193532. The financial support is gratefully acknowledged.

Institutional Review Board Statement: Not applicable.

Informed Consent Statement: Not applicable.

Data Availability Statement: The data that support the findings of this study are available from the corresponding author upon reasonable request.

Acknowledgments: The authors gratefully acknowledge the following researchers and technical staff for their valuable contributions in performing various material characterization analyses:

- Husam Ahmad (Group of Composites and Material Compounds, IWW, TU Chemnitz, Germany) for the SEM and EDX phase analyses;
- Marc Pügner (Group of Materials and Surface Engineering, IWW, TU Chemnitz, Germany) for the XRD analyses;
- Anton Böttcher (Group of Composites and Material Compounds, IWW, TU Chemnitz, Germany) for the light microscopy analyses;
- Felix Schubert (Group of Materials Science, IWW, TU Chemnitz, Germany) for the pull-off adhesion test analyses;
- Christian Wesener (Group of Materials and Surface Engineering, IWW, TU Chemnitz, Germany) for the electroplating of the Zn coating on TWS.

Conflicts of Interest: The authors declare no conflict of interest.

References

1. Kah, P.; Suoranta, R.; Martikainen, J.; Magnus, C. Techniques for joining dissimilar materials: Metals and polymers. *Rev. Adv. Mater. Sci.* **2014**, *36*, 152–164.
2. Lambiase, F.; Scipioni, S.I.; Lee, C.J.; Ko, D.C.; Liu, F. A state-of-the-art review on advanced joining processes for metal-composite and metal-polymer hybrid structures. *Materials* **2021**, *14*, 1890. [CrossRef] [PubMed]
3. Nestler, D.; Trautmann, M.; Zopp, C.; Tröltzsch, J.; Osiecki, T.; Nendel, S.; Wagner, G.; Kroll, L. Continuous Film Stacking and Thermoforming Process for Hybrid CFRP/aluminum Laminates. *Procedia CIRP* **2017**, *66*, 107–112. [CrossRef]
4. Grujicic, M.; Sellappan, V.; Omar, M.A.; Seyr, N.; Obieglo, A.; Erdmann, M.; Holzleitner, J. An overview of the polymer-to-metal direct-adhesion hybrid technologies for load-bearing automotive components. *J. Mater. Process. Technol.* **2008**, *197*, 363–373. [CrossRef]
5. Grujicic, M.; Sellappan, V.; Arakere, G.; Ochterbeck, J.M.; Seyr, N.; Obieglo, A.; Erdmann, M.; Holzleitner, J. Investigation of a polymer-metal inter-locking technology for use in load-bearing automotive components. *Multidiscip. Model. Mater. Struct.* **2010**, *6*, 23–44. [CrossRef]
6. Gwon, T.M.; Kim, J.H.; Choi, G.J.; Kim, S.J. Mechanical interlocking to improve metal-polymer adhesion in polymer-based neural electrodes and its impact on device reliability. *J. Mater. Sci.* **2016**, *51*, 6897–6912. [CrossRef]
7. Bula, K.; Sterzyński, T.; Piasecka, M.; Różański, L. Deformation Mechanism in Mechanically Coupled Polymer–Metal Hybrid Joints. *Materials* **2020**, *13*, 2512. [CrossRef]
8. Paul, H.; Luke, M.; Henning, F. Combining mechanical interlocking, force fit and direct adhesion in polymer–metal-hybrid structures—Evaluation of the deformation and damage behavior. *Compos. Part B Eng.* **2015**, *73*, 158–165. [CrossRef]

9. Lambiase, F. Influence of process parameters in mechanical clinching with extensible dies. *Int. J. Adv. Manuf. Technol.* **2013**, *66*, 2123–2131. [CrossRef]
10. Lee, S.H.; Lee, C.J.; Kim, B.H.; Ahn, M.S.; Kim, B.M.; Ko, D.C. Effect of tool shape on hole clinching for CFRP with steel and aluminum alloy sheet. *Key Eng. Mater.* **2014**, *622–623*, 476–483. [CrossRef]
11. Hahn, O.; Finkeldey, C. Ultrasonic Riveting and Hot-air-sticking of Fiber-reinforced Thermoplastics. *J. Thermoplast. Compos. Mater.* **2003**, *16*, 521–528. [CrossRef]
12. Bula, K.; Korzeniewski, B. Polyamide 6-Aluminum Assembly Enhanced by Laser Micro structuring. *Polymers* **2022**, *14*, 288. [CrossRef] [PubMed]
13. Wurzbacher, S.; Gach, S.; Reisgen, U.; Hopmann, C. Joining of plastic-metal hybrid components by over-molding of specially designed form-closure elements. *Materwiss. Werksttech.* **2021**, *52*, 367–378. [CrossRef]
14. Gebauer, J.; Fischer, M.; Lasagni, A.F.; Kühnert, I.; Klotzbach, A. Laser structured surfaces for metal-plastic hybrid joined by injection molding. *J. Laser Appl.* **2018**, *30*, 032021. [CrossRef]
15. Saborowski, E.; Steinert, P.; Dittes, A.; Lindner, T.; Schubert, A.; Lampke, T. Introducing fractal dimension for interlaminar shear and tensile strength assessment of mechanically interlocked polymer-metal interfaces. *Materials* **2020**, *13*, 2171. [CrossRef] [PubMed]
16. Müller, S.; Brand, M.; Dröder, K.; Meiners, D. Increasing the structural integrity of hybrid plastics-metal parts by an innovative mechanical interlocking effect. *Mater. Sci. Forum* **2015**, *825–826*, 417–424. [CrossRef]
17. Kleffel, T.; Drummer, D. Electrochemical treatment of metal inserts for subsequent assembly injection molding of tight electronic systems. *J. Polym. Eng.* **2018**, *38*, 675–684. [CrossRef]
18. Chan, C.W.; Smith, G.C. Fibre laser joining of highly dissimilar materials: Commercially pure Ti and PET hybrid joint for medical device applications. *Mater. Des.* **2016**, *103*, 278–292. [CrossRef]
19. Fortunato, A.; Cuccolini, G.; Ascari, A.; Orazi, L.; Campana, G.; Tani, G. Hybrid metal-plastic joining by means of laser. *Int. J. Mater. Form.* **2010**, *3* (Suppl. S1), 1131–1134. [CrossRef]
20. Cenigaonaindia, A.; Liébana, F.; Lamikiz, A.; Echegoyen, Z. Novel Strategies for Laser Joining of Polyamide and AISI 304. *Phys. Procedia* **2012**, *39*, 92–99. [CrossRef]
21. Ridder, H.; Schnieders, J. Hybridspritzgießen—Möglichkeiten und Grenzen. In Proceedings of the Tagung Spritzgießen 2007—Oberflächen von Spritzgegossenen Teilen, Hybride Bauteile und Elektromechanik, Baden-Baden, Germany, 14–15 February 2007; VDI Verlag: Düsseldorf, Germany, 2007.